Chapter 1

Nuclear Reactions: Concepts and Cross Sections

> *"A nuclear reaction is a rearrangement of nucleons under the strong interaction. The cross section converts a microscopic probability into a measurable counting rate."*
>
> experimental nuclear physics [6, 1]

Radioactive decay is spontaneous. **Nuclear reactions** are induced: a projectile strikes a target and nucleons are redistributed. This chapter introduces the general notation $a+A \to b+B$, the laboratory setup, a careful definition of the differential cross section, laboratory versus centre-of-mass energies, the Coulomb barrier, reaction types (elastic, inelastic, transfer, capture), and the compound-nucleus versus direct mechanisms with their characteristic timescales and Bohr's independence hypothesis [6, 1, 14, 2].

1.1 General form of a nuclear reaction

A two-body reaction is written

$$a + A \longrightarrow b + B, \tag{1.1}$$

or in compact spectroscopic notation

$$A(a, b)B. \tag{1.2}$$

Here a is the **projectile**, A the **target**, b the detected light product, and B the **residual** (often left in the target). Examples: $^{14}\mathrm{N}(\alpha, p)^{17}\mathrm{O}$, $^{238}\mathrm{U}(n, \gamma)^{239}\mathrm{U}$. If several light particles emerge one writes $A(a, np)B$, and so on [6, 1].

Decay versus reaction. In α or β decay a single parent rearranges spontaneously. In a reaction two nuclei interact because the experimenter supplies a beam (or a neutron flux). Gamma decay changes neither Z nor A; reactions generally do.

1.2 Experimental setup

A typical arrangement is:

(i) an accelerator (or radioactive source, or reactor) that produces a beam of projectiles a with known kinetic energy;

(ii) a thin target containing nuclei A, in vacuum to avoid air scattering;

(iii) one or more detectors that count product particles b in a solid angle $\mathrm{d}\Omega$ at laboratory angle θ, and measure their kinetic energy.

The residual B often stops in the target. The raw data are counts versus energy at each angle: the ingredients of a differential cross section [6, 1].

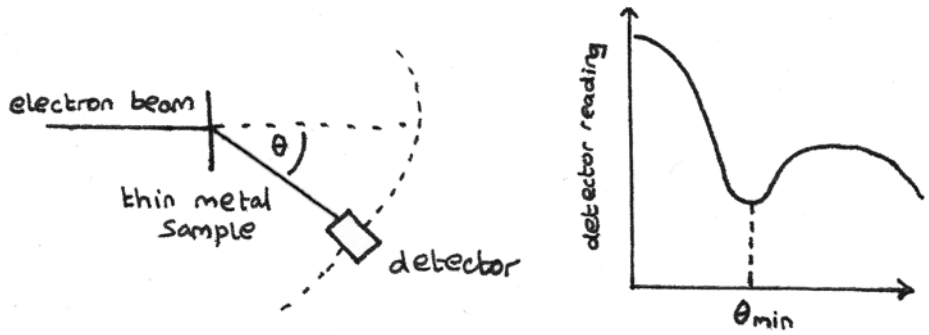

Figure 1.1: Schematic of a fixed-target scattering/reaction experiment: beam, target, and detector at angle θ subtending solid angle $\mathrm{d}\Omega$.

Heavy-ion beams open additional reaction mechanisms; this chapter focuses on light projectiles (n, p, d, α, ...) [14, 2].

1.3 Definition of the cross section

1.3.1 Intensity and counting rate

Let I be the beam **intensity** (number of projectiles per unit area per unit time):

$$I = \frac{\text{number of incident particles}}{\text{unit area} \times \text{unit time}}. \tag{1.3}$$

In a measurement time interval, let $\mathrm{d}N$ be the number of product particles b counted in solid angle $\mathrm{d}\Omega$. Empirically,

$$\mathrm{d}N \propto I, \qquad \mathrm{d}N \propto N_t, \qquad \mathrm{d}N \propto \mathrm{d}\Omega, \tag{1.4}$$

where N_t is the number of target nuclei illuminated by the beam. Introducing a proportionality factor with units of area defines the **differential cross section** $\mathrm{d}\sigma/\mathrm{d}\Omega$:

$$\mathrm{d}N = I\, N_t \frac{\mathrm{d}\sigma}{\mathrm{d}\Omega}\, \mathrm{d}\Omega. \tag{1.5}$$

Equivalently,

$$\frac{\mathrm{d}\sigma}{\mathrm{d}\Omega} = \frac{\mathrm{d}N}{I\, N_t\, \mathrm{d}\Omega}. \tag{1.6}$$

The **total cross section** for a given channel is the integral over all directions:

$$\sigma = \int \frac{\mathrm{d}\sigma}{\mathrm{d}\Omega}\, \mathrm{d}\Omega. \tag{1.7}$$

Physical meaning. The cross section is an effective area: if every projectile that hits a disk of area σ centred on a target nucleus reacted, the observed rate would match experiment. Real quantum scattering is not hard-sphere geometry, but the units remain those of area [6, 1, 14].

1.3.2 Areal density and beam area

If the target has number density n (nuclei per unit volume), thickness t, and the beam spot area is A', then

$$N_t = n\,A'\,t = n_a\,A', \qquad n_a \equiv n\,t \tag{1.8}$$

(n_a: areal density, nuclei per unit area). The number of incident particles per unit time is $N_i = IA'$. Substituting into (1.5),

$$\mathrm{d}N = (IA')\,(nt)\,\frac{\mathrm{d}\sigma}{\mathrm{d}\Omega}\,\mathrm{d}\Omega = N_i\,n_a\,\frac{\mathrm{d}\sigma}{\mathrm{d}\Omega}\,\mathrm{d}\Omega, \tag{1.9}$$

or, when N_t is identified with the areal count in the beam,

$$\mathrm{d}N = I\,n_a\,\frac{\mathrm{d}\sigma}{\mathrm{d}\Omega}\,\mathrm{d}\Omega. \tag{1.10}$$

All of these forms are equivalent once N_t and I are defined consistently [6, 1].

1.3.3 Units: the barn

Because $\mathrm{d}N$ is a pure number and $IN_t\,\mathrm{d}\Omega$ has units of inverse area times solid angle factors already accounted for in the definition, σ has units of **area**. The practical nuclear unit is the barn:

$$1\,\mathrm{b} = 10^{-24}\,\mathrm{cm}^2 = 10^{-28}\,\mathrm{m}^2. \tag{1.11}$$

Typical reaction cross sections range from microbarns to thousands of barns (resonant neutron capture) [6, 1].

Remark

Rutherford scattering already used the same idea: $\mathrm{d}\sigma/\mathrm{d}\Omega$ is the quantity that multiplies flux and target density to give a counting rate. Nuclear reactions generalise that language to all exit channels [2, 14].

1.4 Laboratory and centre-of-mass frames

Theory is simplest in the **centre-of-mass (CM)** frame, where total momentum vanishes. In the laboratory the target is usually at rest. For non-relativistic two-body kinematics with projectile mass m_a, target mass m_A, and laboratory kinetic energy E_{lab},

$$E_{\mathrm{cm}} = \frac{m_A}{m_a + m_A}\,E_{\mathrm{lab}} = \frac{\mu}{m_a}\,E_{\mathrm{lab}}, \tag{1.12}$$

where $\mu = m_a m_A/(m_a + m_A)$ is the reduced mass. Derivation: the CM velocity in the lab is $v_{\rm cm} = m_a v_1/(m_a + m_A)$. In the CM frame the relative speed remains v_1, and

$$E_{\rm cm} = \tfrac{1}{2}\mu v_1^2 = \frac{m_A}{m_a + m_A}\left(\tfrac{1}{2} m_a v_1^2\right) = \frac{m_A}{m_a + m_A}\, E_{\rm lab}. \tag{1.13}$$

Only $E_{\rm cm}$ is available for excitation and reaction Q-value balance; the remainder is locked in CM motion of the system as a whole [6, 1].

The laboratory scattering angle $\theta_{\rm lab}$ and CM angle $\theta_{\rm cm}$ are related (elastic equal-mass special cases aside) by

$$\tan\theta_{\rm lab} = \frac{\sin\theta_{\rm cm}}{\cos\theta_{\rm cm} + m_a/m_A} \tag{1.14}$$

for elastic scattering of a on A (standard textbook form). Angular distributions should always state the frame [6, 14].

1.5 Coulomb barrier

For charged projectiles the long-range force is Coulomb repulsion. At separation r,

$$V_C(r) = \frac{1}{4\pi\varepsilon_0}\frac{Z_a Z_A e^2}{r}. \tag{1.15}$$

Near the nuclear surface $r \approx R_a + R_A \approx r_0(A_a^{1/3} + A_A^{1/3})$ the Coulomb barrier height is of order several MeV for light ions on medium targets, and tens of MeV for heavy systems. Below the barrier, elastic Coulomb (Rutherford) scattering dominates; nuclear reactions require penetration of the barrier (tunnelling) or energies above it. Neutrons feel no Coulomb barrier and can react at thermal energies [6, 1, 2].

At short distance the attractive nuclear potential takes over, producing a pocket that supports compound-nucleus resonances (next chapter and fission lectures).

1.6 Types of processes

1.6.1 Scattering versus reaction

If $a = b$ and $A = B$ as nuclear species, one speaks of **scattering**. If identities change ($a \neq b$ or $A \neq B$), one speaks of a **reaction** in the narrow sense. Both are nuclear reactions in the broad sense [6].

1.6.2 Elastic and inelastic scattering

Elastic scattering leaves A in its ground state. Total kinetic energy is conserved in the CM frame (rest masses unchanged):

$$K_a + K_A = K'_a + K'_A. \tag{1.16}$$

Inelastic scattering excites A (or a) by energy E^*:

$$K_a + K_A = K'_a + K'_A + E^*. \tag{1.17}$$

The detected spectrum shows discrete peaks at kinetic energies reduced by E^* (recoil corrected) [6, 1].

1.6.3 Transfer: stripping and pickup

In a **transfer reaction** one or more nucleons move between projectile and target.

- **Stripping:** the projectile loses a nucleon to the target. Example: (d, p) deposits a neutron; the proton is detected.
- **Pickup:** the projectile gains a nucleon from the target. Example: (p, d) picks up a neutron.

Transfer angular distributions are sensitive to the orbital angular momentum of the transferred nucleon and are a primary tool of nuclear spectroscopy [6, 14].

1.6.4 Capture

In a **capture reaction** the projectile is absorbed and the residual de-excites, often by γ emission: $A(n,\gamma)B$, $A(p,\gamma)B$. Neutron capture on heavy nuclei is central to reactors and nucleosynthesis [6, 1].

1.7 Direct reactions versus compound nucleus

1.7.1 Timescales

Two limiting mechanisms organise most data:

(1) **Direct reactions.** The projectile interacts with one or a few surface nucleons and exits promptly. The characteristic time is the transit time across the nucleus,

$$t_{\text{direct}} \sim \frac{2R}{v} \sim 10^{-22}\,\text{s} \tag{1.18}$$

for $\sim 20\,\text{MeV}$ nucleons ($v \sim 0.2c$, $R \sim 10\,\text{fm}$). Angular distributions are **forward peaked**: memory of the beam direction survives.

(2) **Compound-nucleus (CN) reactions.** The projectile is absorbed; its energy is shared among many nucleons until a quasi-equilibrated excited nucleus C^* forms. Typical lifetimes before particle emission are

$$t_{\text{CN}} \sim 10^{-16}\text{–}10^{-15}\,\text{s}, \tag{1.19}$$

many orders of magnitude longer than t_{direct}. Emission resembles evaporation; in the CM frame the angular distribution is nearly **symmetric** (often nearly isotropic for high level density) [6, 1, 14].

Symbolically,

$$a + A \;\longrightarrow\; C^* \;\longrightarrow\; b + B. \tag{1.20}$$

1.7.2 de Broglie wavelength and energy regime

The projectile de Broglie wavelength (often quoted as the reduced wavelength $\bar{\lambda} = \hbar/p$) sets the spatial scale of the interaction:

$$\bar{\lambda} = \frac{\hbar}{p} = \frac{\hbar c}{\sqrt{2 m_a c^2 \, E}}. \tag{1.21}$$

Using $\hbar c \approx 197\,\mathrm{MeV}\cdot\mathrm{fm}$ and $m_p c^2 \approx 938\,\mathrm{MeV}$, a 10 MeV proton has

$$\bar{\lambda} \approx \frac{197}{\sqrt{2 \times 938 \times 10}} \approx \frac{197}{137} \approx 1.4\,\mathrm{fm}, \tag{1.22}$$

while the full wavelength $h/p = 2\pi\bar{\lambda}$ is a few fm, comparable to a medium nucleus and favourable to CN formation. At $E \sim 40\,\mathrm{MeV}$, $\bar{\lambda} \sim 0.7\,\mathrm{fm}$ approaches nucleon size and direct processes gain weight [6, 1].

1.7.3 Bohr independence hypothesis

Bohr's **independence hypothesis** states that once C^* is formed at a given excitation energy (and spin, parity), it forgets the entrance channel. Decay branching ratios depend only on the properties of C^*, not on whether C^* was made by $p + A$ or $\alpha + A'$.

Classic test: Ghoshal's experiment comparing

$$p + {}^{63}\mathrm{Cu} \to {}^{64}\mathrm{Zn}^* \to \text{various exit channels} \tag{1.23}$$

with

$$\alpha + {}^{60}\mathrm{Ni} \to {}^{64}\mathrm{Zn}^* \to \text{same exit channels}. \tag{1.24}$$

When laboratory energies are matched so that the excitation energy of ${}^{64}\mathrm{Zn}^*$ is the same, the excitation functions $\sigma(E)$ for identical exit channels nearly coincide [6, 1].

Matching excitation energies. In the CM frame, absorption of a proton on ${}^{63}\mathrm{Cu}$ gives

$$\Delta E = (m_p + m_{\mathrm{Cu}} - m_{\mathrm{Zn}})c^2 + K_p\Big(1 + \frac{m_p}{m_{\mathrm{Cu}}}\Big), \tag{1.25}$$

so the laboratory kinetic energy needed for a chosen ΔE is

$$K_p = \frac{\Delta E - (m_p + m_{\mathrm{Cu}} - m_{\mathrm{Zn}})c^2}{1 + m_p/m_{\mathrm{Cu}}}. \tag{1.26}$$

An analogous formula with $(m_\alpha, m_{\mathrm{Ni}})$ replaces (m_p, m_{Cu}) for the α channel. Different mass combinations imply different laboratory energy scales for the same ΔE, which is why Ghoshal plots use two shifted energy axes [6].

Bohr compound nucleus (1936)

Niels Bohr proposed that low-energy nuclear reactions proceed through a long-lived intermediate nucleus in statistical equilibrium. The picture explains dense resonances, nearly isotropic evaporation spectra, and entrance-channel independence. Direct reactions (Butler, Austern, ...) emerged later as the complementary short-timescale limit [6, 14, 2].

Key idea

Students should remember:

- Reaction: $a + A \to b + B$ or $A(a, b)B$.
- $\mathrm{d}N = IN_t(\mathrm{d}\sigma/\mathrm{d}\Omega)\,\mathrm{d}\Omega$; I = particles per unit area per unit time.
- σ has units of area; $1\,\mathrm{b} = 10^{-24}\,\mathrm{cm}^2$.
- $E_{\mathrm{cm}} = m_A E_{\mathrm{lab}}/(m_a + m_A)$.
- Elastic vs inelastic; stripping/pickup; capture; Coulomb barrier for charged beams.
- Direct $\sim 10^{-22}\,\mathrm{s}$, forward peaked; CN $\sim 10^{-16}$–$10^{-15}\,\mathrm{s}$, more isotropic; Bohr independence.

1.8 Further physics from the literature

Optical model and elastic scattering. Elastic scattering of nucleons is described by a complex optical potential whose imaginary part accounts for absorption into non-elastic channels. The resulting diffraction patterns and reaction cross sections connect to the total cross section via the optical theorem [6, 14, 2].

DWBA for transfer. Direct stripping and pickup are analysed with the distorted-wave Born approximation (DWBA). Angular distributions determine the transferred orbital angular momentum ℓ; spectroscopic factors measure single-particle occupation relative to a pure shell-model configuration [6, 14].

Hauser–Feshbach theory. Statistical CN decay is computed with Hauser–Feshbach theory: transmission coefficients for all open channels, spin and parity conservation, and level densities. Bohr independence is built in by construction [6, 1].

Heavy-ion reactions. Heavy projectiles open fusion, deep-inelastic scattering, and multi-nucleon transfer. Timescales and angular distributions again separate quasi-elastic direct processes from long-lived fused systems [14, 2].

Reading guide

Krane [6] Ch. 11–12 (reactions, compound nucleus, direct reactions); Dunlap [1] (cross sections and experimental methods); Basdevant [14] (mechanisms); Demtröder [2] (accelerators and detectors). Ghoshal's classic comparison is discussed in standard reaction chapters of Krane and Blatt–Weisskopf.

1.9 Problems with solutions

Problem 21.1: Differential cross section from counts

A beam of intensity $I = 2.0 \times 10^{10}\,\mathrm{cm^{-2}\,s^{-1}}$ illuminates $N_t = 1.5 \times 10^{19}$ target nuclei. In $\Delta t = 100\,\mathrm{s}$, a detector with $\Delta\Omega = 5.0 \times 10^{-3}\,\mathrm{sr}$ records $N = 3.0 \times 10^{4}$ product particles (assume $\mathrm{d}\sigma/\mathrm{d}\Omega$ constant over the detector). Find $\mathrm{d}\sigma/\mathrm{d}\Omega$ in mb/sr [6, 1].

Solution 21.1

From $\mathrm{d}N = I N_t (\mathrm{d}\sigma/\mathrm{d}\Omega)\,\mathrm{d}\Omega$ integrated over the run,

$$N = I N_t \frac{\mathrm{d}\sigma}{\mathrm{d}\Omega}\Delta\Omega\,\Delta t.$$

$$\frac{\mathrm{d}\sigma}{\mathrm{d}\Omega} = \frac{N}{I N_t\,\Delta\Omega\,\Delta t} = \frac{3.0 \times 10^{4}}{(2.0 \times 10^{10})(1.5 \times 10^{19})(5.0 \times 10^{-3})(100)} = \frac{3.0 \times 10^{4}}{1.5 \times 10^{30}} = 2.0 \times 10^{-26}\,\mathrm{cm^2/sr}.$$

Since $1\,\mathrm{b} = 10^{-24}\,\mathrm{cm^2}$,

$$\frac{\mathrm{d}\sigma}{\mathrm{d}\Omega} = 0.020\,\mathrm{b/sr} = 20\,\mathrm{mb/sr}.$$

Problem 21.2: Areal density

A gold foil ($A = 197$, density $\rho = 19.3\,\mathrm{g\,cm^{-3}}$) has thickness $t = 2.0\,\mu\mathrm{m}$. Estimate the areal density $n_a = nt$ in nuclei per $\mathrm{cm^2}$. Use $N_A = 6.02 \times 10^{23}\,\mathrm{mol^{-1}}$ [1].

Solution 21.2

Number density

$$n = \frac{\rho N_A}{A} = \frac{19.3 \times 6.02 \times 10^{23}}{197} = 5.90 \times 10^{22}\,\mathrm{cm^{-3}}.$$

$$t = 2.0 \times 10^{-4}\,\mathrm{cm}, \qquad n_a = nt = 1.18 \times 10^{19}\,\mathrm{cm^{-2}}.$$

Problem 21.3: Lab to CM energy

A 12.0 MeV proton beam strikes a stationary ^{12}C target. Find E_{cm}. What fraction of E_{lab} is unavailable for excitation? [6]

Solution 21.3

$$E_{\mathrm{cm}} = \frac{m_C}{m_p + m_C} E_{\mathrm{lab}} \approx \frac{12}{13} \times 12.0\,\mathrm{MeV} = 11.08\,\mathrm{MeV}.$$

Unavailable fraction (CM motion):

$$\frac{m_p}{m_p + m_C} = \frac{1}{13} \approx 7.7\%.$$

Problem 21.4: Coulomb barrier estimate

Estimate V_C at contact for $\alpha + {}^{208}\mathrm{Pb}$ using $R = 1.2(A_\alpha^{1/3} + A_{\mathrm{Pb}}^{1/3})\,\mathrm{fm}$ and $e^2/(4\pi\varepsilon_0) = 1.44\,\mathrm{MeV}\cdot\mathrm{fm}$ [6, 1].

Solution 21.4

$$R = 1.2(4^{1/3} + 208^{1/3}) = 1.2(1.59 + 5.92) = 9.01\,\mathrm{fm}.$$

$$V_C = \frac{(2)(82)(1.44)}{9.01} = \frac{236.2}{9.01} \approx 26.2\,\mathrm{MeV}.$$

An α beam well below $\sim 26\,\mathrm{MeV}$ (lab, with CM correction) interacts mainly by Coulomb scattering unless it tunnels.

Problem 21.5: Direct transit time

Estimate the transit time of a 20 MeV proton across a nucleus of diameter 10 fm. Use non-relativistic kinematics with $m_p c^2 \approx 938\,\mathrm{MeV}$ [6].

Solution 21.5

$$\tfrac{1}{2}mv^2 = 20\,\mathrm{MeV} \quad \Rightarrow \quad \frac{v}{c} = \sqrt{\frac{2K}{mc^2}} = \sqrt{\frac{40}{938}} \approx 0.206.$$

$$t = \frac{10\,\mathrm{fm}}{0.206\,c} = \frac{10 \times 10^{-15}\,\mathrm{m}}{0.206 \times 3.00 \times 10^{8}\,\mathrm{m\,s^{-1}}} \approx 1.6 \times 10^{-22}\,\mathrm{s}.$$

This matches the direct-reaction timescale $\sim 10^{-22}\,\mathrm{s}$.

Problem 21.6: Classify the process

Classify each as elastic, inelastic, stripping, pickup, or capture [6, 1]:

(a) ${}^{40}\mathrm{Ca}(p,p){}^{40}\mathrm{Ca}$ (g.s. to g.s.);

(b) ${}^{40}\mathrm{Ca}(p,p'){}^{40}\mathrm{Ca}^*$;

(c) ${}^{40}\mathrm{Ca}(d,p){}^{41}\mathrm{Ca}$;

(d) ${}^{40}\mathrm{Ca}(p,d){}^{39}\mathrm{Ca}$;

(e) ${}^{40}\mathrm{Ca}(n,\gamma){}^{41}\mathrm{Ca}$.

Solution 21.6

(a) Elastic scattering.
(b) Inelastic scattering.
(c) Stripping (deuteron loses a neutron).
(d) Pickup (proton gains a neutron).
(e) Radiative capture.

Problem 21.7: Bohr independence

Two entrance channels form the same compound nucleus C^* at the same excitation energy and spin. What does Bohr independence predict for the relative yields of two exit channels $b_1 + B_1$ and $b_2 + B_2$? Why must laboratory energies differ for $p + A$ versus $\alpha + A'$? [6]

Solution 21.7

Independence predicts that branching ratios (relative partial widths) of C^* are the same regardless of entrance channel. Absolute cross sections still contain an entrance formation factor, but excitation functions for a given exit channel should match when plotted versus excitation energy of C^*.

Laboratory energies differ because the Q-value for forming C and the mass ratios in $E_{\mathrm{cm}} = m_A K_a/(m_a + m_A)$ differ for (p, A) and (α, A'). Matching ΔE requires different K_a scales (Ghoshal plot with two energy axes).

Bibliography

[1] R. A. Dunlap, *An Introduction to the Physics of Nuclei and Particles* (2nd ed.), IOP Publishing, Bristol (2023), DOI: 10.1088/978-0-7503-6094-4, Ch. 3 (Nuclear composition and size).

[2] W. Demtröder, *Nuclear and Particle Physics*, Undergraduate Lecture Notes in Physics, Springer, Cham (2023).

[3] S. Petrera, *Problems and Solutions in Nuclear and Particle Physics*, UNITEXT for Physics, Springer, Cham (2019).

[4] F. Terranova, *A Modern Primer in Particle and Nuclear Physics*, Oxford University Press (2021).

[5] S. D'Auria, *Introduction to Nuclear and Particle Physics*, Undergraduate Lecture Notes in Physics, Springer, Cham (2018).

[6] K. S. Krane, *Introductory Nuclear Physics*, Wiley, New York (1988).

[7] R. Hofstadter, "Electron scattering and nuclear structure," Rev. Mod. Phys. **28**, 214 (1956).

[8] H. F. Ehrenberg, R. Hofstadter, U. Meyer-Berkhout, D. G. Ravenhall, and S. E. Sobottka, "High-Energy Electron Scattering and the Charge Distribution of Carbon-12 and Oxygen-16," Phys. Rev. **113**, 666 (1959).

[9] H. Yukawa, "On the interaction of elementary particles. I," Proc. Phys.-Math. Soc. Japan **17**, 48 (1935).

[10] R. D. Woods and D. S. Saxon, "Diffuse surface optical model for nucleon-nuclei scattering," Phys. Rev. **95**, 577 (1954).

[11] H. G. J. Moseley, "The high-frequency spectra of the elements," Phil. Mag. **26**, 1024 (1913); **27**, 703 (1914).

[12] C. F. von Weizsäcker, "Zur Theorie der Kernmassen," Z. Phys. **96**, 431 (1935).

[13] P. Cappellaro, *Introduction to Applied Nuclear Physics* (MIT OpenCourseWare / LibreTexts), CC BY-NC-SA 4.0.

[14] J.-L. Basdevant, J. Rich, and M. Spiro, *Fundamentals in Nuclear Physics: From Nuclear Structure to Cosmology*, Springer, New York (2005).

[15] D. Tong, *Particle Physics*, Lecture notes (University of Cambridge / CERN school notes).

[16] M. G. Mayer, "On closed shells in nuclei. II," Phys. Rev. **75**, 1969 (1949).

[17] O. Haxel, J. H. D. Jensen, and H. E. Suess, "On the "magic numbers" in nuclear structure," Phys. Rev. **75**, 1766 (1949).

[18] T. Schmidt, "Über die magnetischen Momente der Atomkerne," Z. Phys. **106**, 358 (1937).

[19] L. W. Nordheim, "On spins, moments, and shells in nuclei," Phys. Rev. **78**, 294 (1950).

[20] Evaluated Nuclear Structure Data File (ENSDF), National Nuclear Data Center, Brookhaven National Laboratory, `https://www.nndc.bnl.gov/ensdf/`.

[21] NuDat 3, National Nuclear Data Center, Brookhaven National Laboratory, `https://www.nndc.bnl.gov/nudat3/`.

[22] N. J. Stone, "Table of nuclear magnetic dipole and electric quadrupole moments," At. Data Nucl. Data Tables **90**, 75 (2005); updated compilations at NNDC.

[23] W. N. Cottingham and D. A. Greenwood, *An Introduction to Nuclear Physics* (2nd ed.), Cambridge University Press, Cambridge (2001).

[24] H. Geiger and J. M. Nuttall, "The ranges of the α particles from the radioactive substances," Phil. Mag. **22**, 613 (1911).

[25] G. Gamow, "Zur Quantentheorie des Atomkernes," Z. Phys. **51**, 204 (1928).

[26] R. W. Gurney and E. U. Condon, "Wave mechanics and radioactive disintegration," Nature **122**, 439 (1928); Phys. Rev. **33**, 127 (1929).

[27] M. Wang, W. J. Huang, F. G. Kondev, G. Audi, and S. Naimi, "The AME 2020 atomic mass evaluation (II). Tables, graphs and references," Chin. Phys. C **45**, 030003 (2021).

[28] Laboratoire National Henri Becquerel (LNHB), Recommended decay data, `http://www.lnhb.fr/nuclear-data/nuclear-data-table/`.

[29] L. M. Langer, R. D. Moffat, and H. C. Price, Jr., "Low energy beta-ray spectra: P^{32} and Cu^{64}," Phys. Rev. **76**, 1725 (1949).

[30] L. M. Langer and H. C. Price, Jr., "Shapes of the beta-spectra of the forbidden transitions of Sb^{124}, Rb^{86}, Sr^{89}, Y^{91}, and Cs^{137}," Phys. Rev. **75**, 1769 (1949).

[31] D. C. Camp and L. M. Langer, "The shape of the ^{66}Ga positron spectrum and the contribution from $0^+ \to 0^+$ transitions," Phys. Rev. **129**, 1782 (1963).